M4E.003

J. N. Nilchi, R. Liu, and C. T.-C. Nguyen, "7th order sharp-roll-off bridged micromechanical filter," *Proceedings* of the 18th Int. Conf. on Solid-State Sensors, Actuators, & Microsystems (Transducers'15), Anchorage, Alaska, June 21-25, 2015, pp. 137-140.

7TH ORDER SHARP-ROLL-OFF BRIDGED MICROMECHANICAL FILTER

J. Naghsh Nilchi, R. Liu, and C.T.-C. Nguyen
Berkeley Sensor and Actuator Center
University of California, Berkeley, Berkeley, CA, USA

ABSTRACT

A 7th-order capacitive-gap transduced 8-MHz micromechanical filter has been demonstrated with a channel-selecting bandwidth of 24 kHz (0.3%) and a shape factor of 1.45, which bests the previous mark of 1.86 for similar frequency MEMS-based filters. This shape factor arises from not only the sheer order of the filter, governed by seven coupled clamped-clamped beam resonators, but also from strategic bridging of its non-adjacent 1st, 4th , and 7th resonators to generate loss poles that further steepen the roll-off from passband to stopband. Interestingly, it is the extremely strong electromechanical coupling on the order of $k^2_{eff} \sim (C_x/C_0) \sim 17\%$ offered by capacitive-gap transduction at HF that allows the use of so many resonators, thereby enabling this filter. The steepness of this filter's roll-off greatly increases the density of available channels in HF radios for military and Ham applications, as well as future sensor network applications enabled by these results.

KEYWORDS

Communications, high-order filter, channel selection, RF front-end, shape factor, insertion loss.

INTRODUCTION

Small frequency filters with millimeter dimensions are quite common in hand-held wireless devices (e.g., cell phones) that operate at UHF frequencies, often in the GHz range. They are in fact key enablers for such ubiquitous applications, since their ability to remove unwanted interfering signals lowers the power consumption of any receiver front-end. Unfortunately, filters of similar size are more difficult to construct for the much lower HF range, spanning frequencies from 3-30MHz, since wavelengths (acoustic or electrical) are much larger at these frequencies. To further complicate matters, the piezoelectric technologies normally employed for GHz filters lack the electromechanical coupling strength to support high-order filters at HF [1, 2, 3, 4].

The availability of high-order filters in millimeter sizes at HF, if possible, would likely spur vibrant activity in not only military and Ham radios, but also in a much bigger ultra-low power sensor network arena, especially if dense packing of channels becomes possible. Pursuant to enabling such a vision, this work uses capacitive-gap transduced beam resonators with individual resonator Q's on the order of 12,000 to demonstrate a 7th-order 8-MHz micromechanical filter, shown in Fig. 1 and Fig. 5, with a channel-selecting bandwidth as small as 24 kHz (0.3%) and a shape factor of 1.45, both of which enable increased channel density at HF.

MICROMECHANICAL FILTER DESIGN

Fig. 1 presents the perspective view schematic of the demonstrated filter. As shown, this filter comprises seven clamped-clamped beam (CC-beam) flexural-mode resonators linked by numerous flexural-mode coupling beams to generate a 14-pole inverse Chebyshev filter response with two loss poles that steepen the transition between pass- and stop-bands. Capacitive-gap transducer electrodes underlie not only the input/output resonators at the ends, but also all resonators in between for which they provide a means to tune frequencies towards a more perfect passband [5].

Fig. 1 also shows a preferred excitation and detection scheme, where dc voltages charge up electrode-to-resonator capacitances to either enhance electromechanical coupling or tune frequencies; an ac input voltage drives the leftmost resonator through a proper termination impedance; and the motional output current drives a transimpedance low-noise

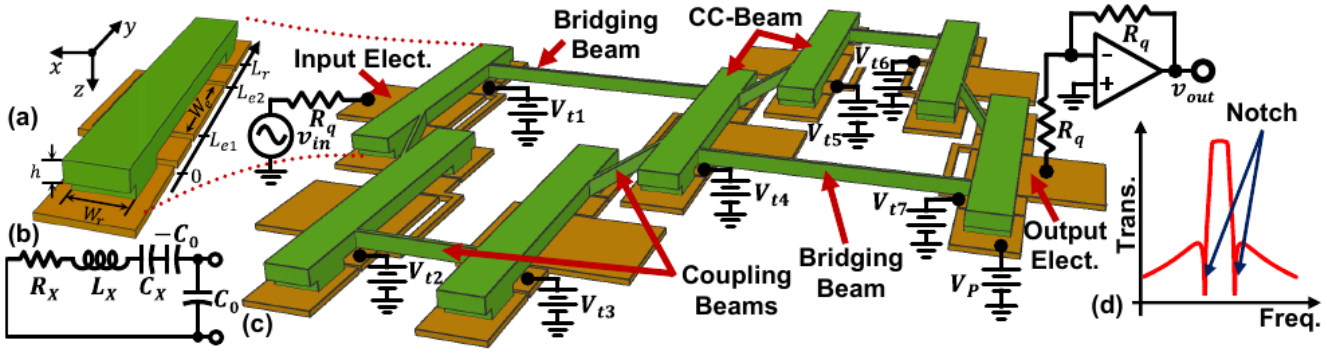

Figure 1: (a) Single clamped-clamped beam (CC-Beam) resonator and (b) its electrical equivalent circuit model. (c) Perspective-view schematic and measurement circuitry for the 7th-order μmechanical filter with bridging between the 1st, 4th and 5th resonators. Tuning electrodes under each resonator allow precise placement of poles and zeros to achieve a sharp passband-to-stopband roll-off (d).

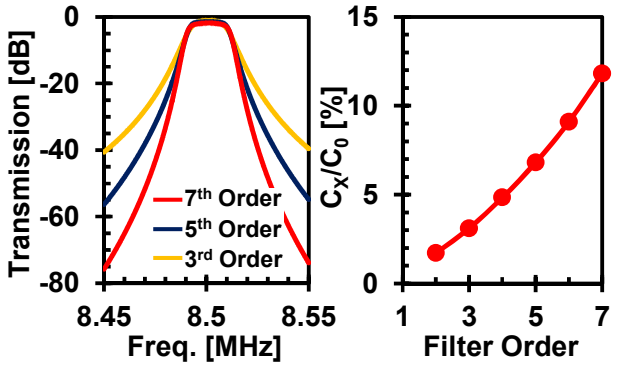

Figure 2: Higher-order filters provide sharper roll-off and larger stopband rejection (left) but they require larger C_x/C_0 for the same termination resistance and bandwidth.

amplifier through output termination impedance R_q.

Electromechanical Coupling Requirements

Attaining a channel-selecting response requires not only constituent resonators with high Q to reduce in-band insertion loss, but also end resonators with high electromechanical coupling to increase stopband rejection and decrease termination resistance. A high order design, where order equates to number of resonators, is also desirable, since it steepens the passband-to-stopband roll-off and increases stopband rejection, as shown in Fig. 2(left). Every added resonator, however, comes at a price, as higher-order generally demands larger electromechanical coupling (C_x/C_o) to suppress passband distortion. Fig. 2(right) presents curves that illustrate how (C_x/C_o) must increase to service a given filter order.

To understand the present approach to tiny, high-order HF filters, one must first dispel the common misconception that capacitive-gap transducers are weak [1]. They are in fact not weak; rather, merely frequency dependent. In particular, the expression for (C_x/C_0) for the CC-beam resonator shown in Fig. 1(a)-(b) takes the form

$$\frac{C_x}{C_0} \approx \frac{\epsilon_0 V_P^2}{\rho h W_e} \frac{1}{d_0^3} \frac{1}{\omega_0^2} \frac{\left(\int_{L_{e1}}^{L_{e2}} X_{mode}(y)dy\right)^2}{\int_0^{L_r} \left(X_{mode}(y)\right)^2 dy} \qquad (1)$$

where V_P, W_e, h, d_0, ω_0, ρ and X_{mode} are dc-bias voltage, electrode width, resonator thickness, gap spacing, radian resonance frequency, density of the structural material, and resonator mode shape function, respectively [5]. Fig. 3(a) plots (C_x/C_o) of a CC-beam biased at a constant 25V as a function of its resonance frequency, showing an impressive 16.7% at 10 MHz, but dropping to 0.66% at 50 MHz.

If one lifts the constant V_P restriction, then the drop in (C_x/C_o) becomes much more gradual, or even disappears. In particular, the best case (i.e., highest permissible value of) dc-bias voltage is the pull-in voltage, which increases with frequency according to

$$V_{pull\_in} = \sqrt{\alpha \frac{k_{re} d_0^3}{\epsilon_0 A_0}} \propto \sqrt{k_{re}} \propto \omega_0 \qquad (2)$$

as shown in Fig. 3(b). Use of $V_{pull,in}$ in (1) yields (C_x/C_o) curves like those in Fig. 3(c), which are now flat with frequency, with large values >15% across the plotted frequency range. Whether or not a voltage as high as 600V for 50 MHz is practical in a real application, 25V at 10 MHz is practical. So if not at GHz frequency, capacitive-gap transducers easily best AlN piezoelectric transducers in the HF range, and by rather large margins, e.g., 16.7% vs. 1%.

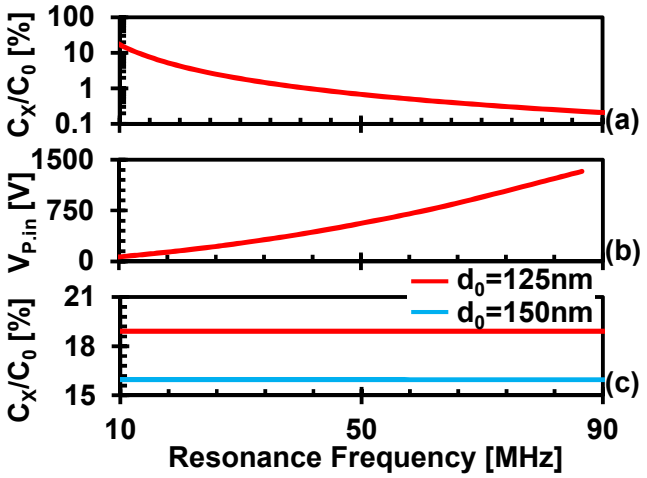

Figure 3: Electromechanical coupling for V_P=25V and d_0=125nm, b) resonator pull-in voltage, and c) electromechanical coupling for V_P=0.75V_{pull_in}, all versus CC-beam resonance frequency.

Armed with this insight, the filter design of Fig. 1 employs capacitive-gap transducers with resonator-to-electrode gap spacing of 137nm, which with a dc bias of 22.5V applied to the beams achieves a very large (C_x/C_0)~17%.

Bridged Coupling

Like previous lower-order micromechanical filters [5] [6], the resonators comprising the present filter are identical in all respects, mainly to harness the better matching than absolute tolerances typical of planar wafer-level fabrication processes. When all resonators are identical, they share the same uncoupled resonance frequency, which becomes the center frequency of the filter response. It is then up to the coupling beams to pull frequencies apart to form a passband around this center frequency [5]. When given quarter-wavelength dimensions, the beams connecting adjacent resonators do just this while contributing (ideally) no effective mass to the resonators themselves, thereby allowing a design where all resonators are identical [5]. This adjacent resonator coupling is similar to that used in previous designs, with the main difference being the larger number of resonators that steepen the roll-off from pass- to stop-band. As in the design of [5], all coupling beams attach to the vertical CC-beam resonators at specifically designed locations that govern the overall filter response, e.g., Chebyshev, Butterworth, etc.

To affect even greater roll-off, the design of Fig. 1 employs bridging beams that couple non-adjacent resonators and introduce loss poles [6] that further shape the response. As shown by color in Fig. 5, bridging introduces a signal path in parallel with that of the series adjacent-coupled one

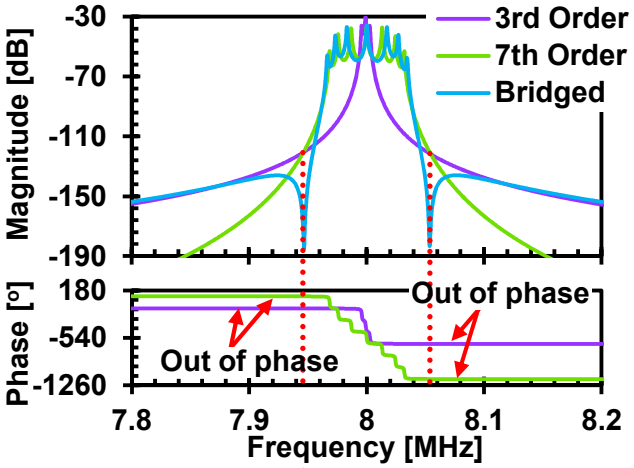

Figure 4: Unterminated 3rd-order, 7th-order, and bridged 7th-order filter magnitude and phase frequency responses, illustrating the formation of loss poles.

that with proper phasing leads to subtraction of signals from the different paths, producing a zero in the transfer function. For the filter of Fig. 1 and Fig. 5, the main signal path (in green) passes through all resonators and λ/4 adjacent-coupling beams to generate the 7th-order filter response shown in green in Fig. 4; while the parallel signal path (in purple) goes through the 1st, 4th and 7th resonators bridged by 3λ/4 coupling beams to create the 3rd-order filter response shown in purple in Fig. 4. The figure further shows that 3λ/4 coupling is 180° out of phase relative to λ/4 coupling at frequency far from center. This means the two signals, once combined, subtract at frequencies far from center, introducing notches in the filter transfer function at frequencies where they have the same magnitude, and sharpening the filter roll-off as shown in blue. In essence, λ/4 coupling sets the bandwidth of the 7th-order filter, while 3λ/4 coupling sets the bandwidth and roll-off of a 3rd-order filter response that subtracts from the former to set loss pole location, and in turn, the 20dB shape factor of the filter.

Tuning via Electrical Stiffness

Achieving very sharp roll-off along with small insertion loss and small in-band ripple requires precise placement of poles and especially zeros. Although the matching tolerance of surface micromachining technology is fairly good [7], it is not sufficient for filters with percent bandwidths below 0.5%. Fortunately, capacitive-gap transducers offer frequency tuning via voltage-controlled electrical stiffness, as governed by

$$f_0 = f_{nom}\sqrt{1-\langle\frac{k_e}{k_m}\rangle} \approx f_{nom}\sqrt{1-\left(\frac{C_x}{C_0}\right)} = f_{nom}\sqrt{1-\gamma V_t^2} \quad (3)$$

where f_0, f_{nom}, k_e, k_m and γ are the overall resonator center frequency, its pure mechanical resonance frequency, its electrical stiffness, its mechanical stiffness, and a transduction constant derived from (1), respectively. Equation (3) predicts a large tuning range on the order of 200ppm for a 1V change in bias voltage for the CC-beam design used here. This tuning capability outright enables the high-order

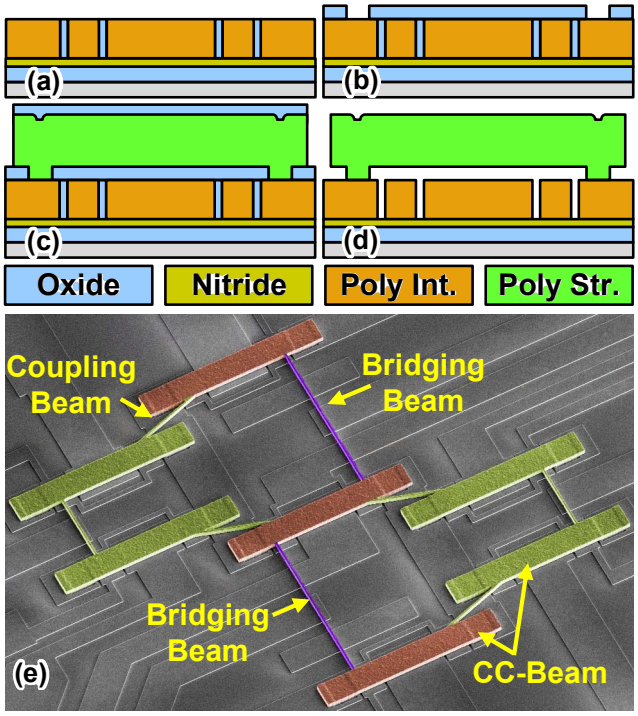

Figure 5: Cross-sections of the fabrication process flow used for the 7th-order bridged filter of this work and colored SEM picture of a fabricated device. The adjacent-coupled and bridged paths are colored green and purple, respectively, and brown resonators are shared between the two.

narrow-band capacitive-gap filter of this work, as without tuning, poles and zeros will miss their marks for such a small filter bandwidth. As shown in Fig. 1, tuning electrodes underlie all seven resonators to achieve maximum tuning ability.

EXPERIMENTAL RESULTS

The 7th-order bridged filter was fabricated using a previously described vertical gap surface-micromachining technology [5], summarized by the process cross-sections of Fig. 5, with added damascene-like steps to realize a thicker-than-usual doped-polysilicon interconnect layer that greatly reduces series resistance. The damascene process realizes the thick patterned polysilicon layer show in Fig. 5(a) while eliminating topography before structural layer steps. Fig. 5 already presented the SEM of a finished 7th order filter, while Table 1 summarizes its design and performance.

Fig. 6 presents the frequency response of the 7th-order bridged Chebyshev filter of Fig. 5(e) terminated by 20kΩ board-level resistors, frequency-tuned using dc-bias voltages under 3V, and measured under 1mTorr in a custom-built vacuum chamber. The required termination resistance R_q depends on the filter percent bandwidth and the motional resistance R_x of the constituent resonators [5]. Although use of wider resonators, or arrays of them, could reduce the needed R_q, this might not be advisable given the advantages of high-impedance in emerging low-power nano-scale wireless communication systems [8]. As shown, the filter achieves an impressive insertion loss of 1.6dB with less than

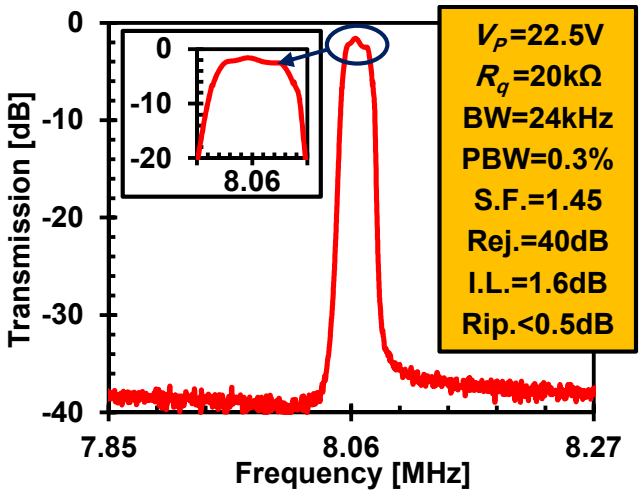

Figure 6: Measured frequency characteristic for the 7th-order bridged micromechanical filter of Fig. 5. The inset zooms in on the filter passband.

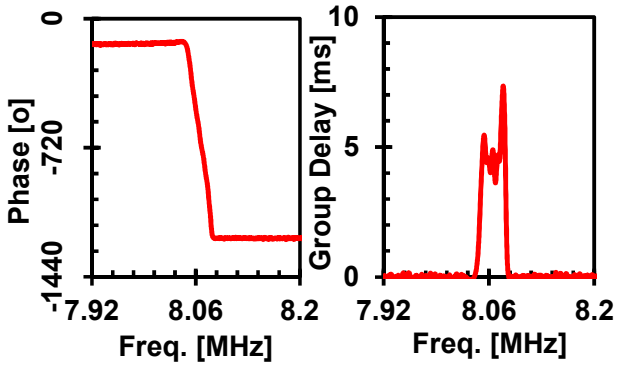

Figure 7: Measured phase response (left) and group delay response (right) for the terminated filter of Fig. 5.

0.5dB of in-band ripple for a 0.3% bandwidth centered at 8.06MHz. Here, low-resistance interconnects helped to reduce the insertion loss of the properly-terminated filter. This filter response exhibits 40dB of out-of-band rejection and a 20dB shape factor of 1.45, which bests the previous mark of 1.86 for a similar frequency MEMS-based filter [1]. Such a sharp roll-off provides excellent rejection of adjacent channels, which could then pack with higher density. The tiny shape factor confirms both the utility of high filter order and the efficacy of non-adjacent resonator bridging.

Fig. 7 presents the measured phase and group delay responses of the terminated filter, showing over 1260° of phase change consistent with the order of the filter and a group delay ripple of 0.5ms. This value is commensurate with the needs of narrowband communication receivers, which unlike wideband ones, can tolerate larger group delays without degradation in system characteristics, e.g., bit error rate.

CONCLUSIONS

The use of a large number of resonators and bridged coupling of non-adjacent ones, together with voltage-controlled electrical stiffness frequency tuning, has allowed sufficient control of pole and loss pole locations to permit the 7th-order micromechanical filter of this work to achieve a shape factor as small as 1.45, while still posting an insertion loss of 1.6dB for a 0.3% bandwidth. The filter further occupies an area of only 0.02mm^2, much smaller than commercially available centimeter-sized filters. This, together with the aforementioned characteristics, stands to not only increase the density of available channels in HF radios, but also enable emerging technologies aimed at the ultra-low power sensor network arena, e.g., the internet of things.

Table 1: HF Micromechanical Filter Summary.

Parameter	Design/Meas.
μRes. Beam Length, L_r	40.8μm
μRes. Beam Width, W_r	8.0μm
μRes. Beam Thickness, h	2.0μm
Electrode Width, W_e	20μm
Gap Spacing, d_0	137nm
Coupling Beam Length, L_{s12}	22.3μm
Coupling Beam Length, L_{s14}	51.8μm
Coupling Beam Width, W_s	0.75μm
Coupling Location, l_{c12}	4.7μm
Coupling Location, l_{c14}	3.2μm
Center Frequency, f_0	8.06MHz
Filter Biasing Voltage, V_P	22.5V
Electromechanical Coupling, C_x/C_0	16.96%
Resonator Quality Factor, Q	12,000
Bandwidth, B	24.3kHz
Percent Bandwidth, B/f_0	0.3%
Passband Ripple, PR	<0.5dB
Insertion Loss, IL	1.6dB
20dB Shape Factor,	1.45
Stopband Rejection, SR	40dB

Acknowledgment. This work was funded by DARPA.

REFERENCES

[1] B. Kim *et al*, "AlN Microresonator-Based Filters ...," *JMEMS,* vol. 22, no. 4, pp. 949-961, 2013.

[2] K. Wang *et al*, "21.7 A 1.8mW PLL-free channelized 2.4GHz ZigBee receiver ...," in *ISSCC*, San Francisco, 2014.

[3] C. Zuo *et al*, "Very high frequency channel-select ...," *Sensors and Actuators A,* vol. 160, no. 1-2, pp. 132-140, 2010.

[4] R. Olsson *et al*, "VHF and UHF mechanically coupled aluminum nitride MEMS filters," in *IFCS*, Honolulu, 2008.

[5] F. Bannon *et al*, "High-Q HF microelectromechanical filters," *JSSC,* vol. 35, no. 4, pp. 512-526, 2000.

[6] S.-S. Li *et al*, "Bridged micromechanical filters," *IFCS*, 2004.

[7] Y. Lin *et al*, "Effect of Electrode Configuration on the Frequency and Quality Factor …," *Transducers*, 2007.

[8] R. Azadegan, *Highly Miniaturized Antennas and Filters ...,* Ph.D. Dissertation, Univ. of Michigan, Ann Arbor, MI, 2004.

CONTACT

*J. Naghsh Nilchi: jalal.naghsh.nilchi@berkeley.edu